Soft Matter

www.rsc.org/softmatter

Volume 9 | Number 4 | 28 January 2013 | Pages 971–1382

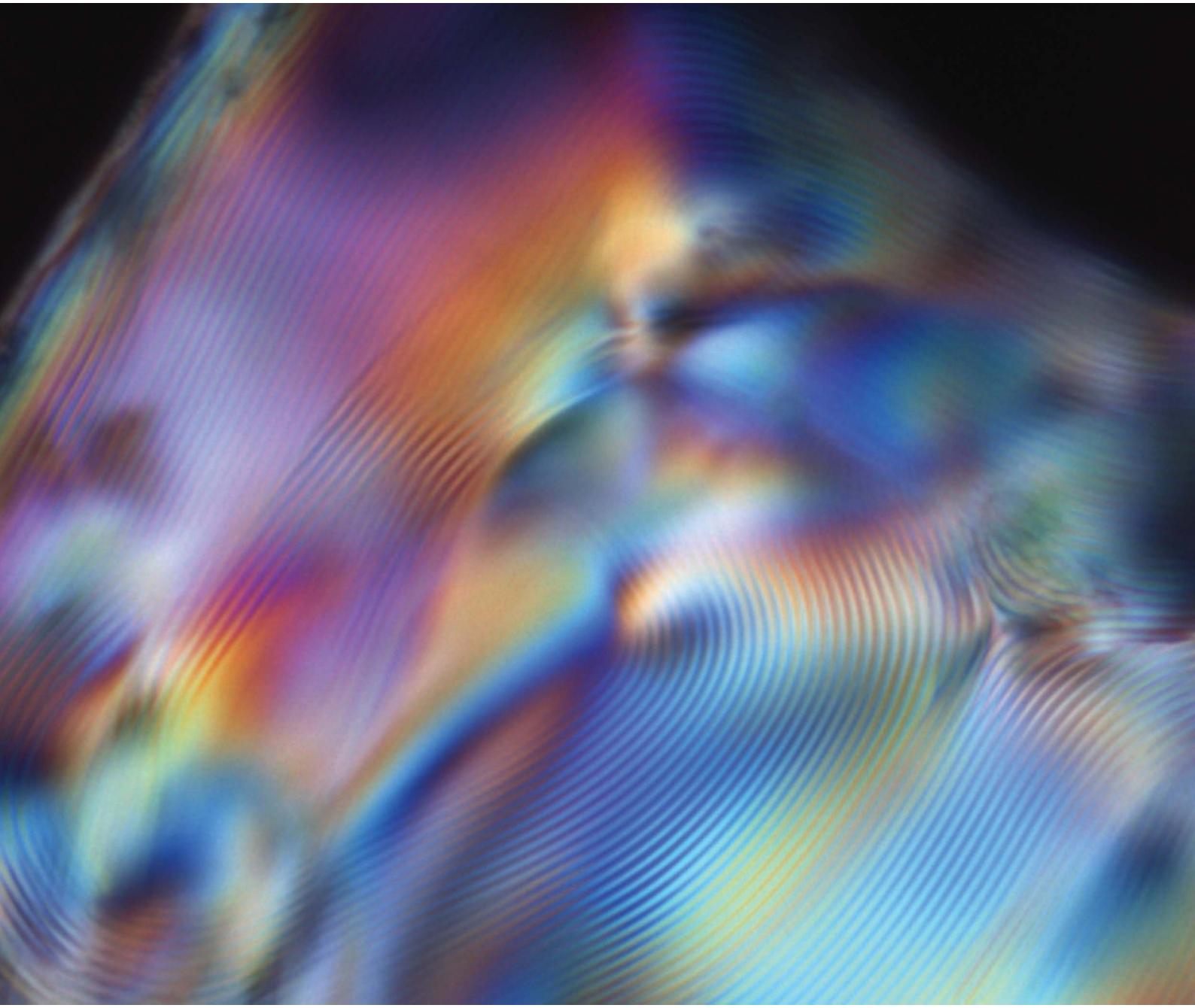

ISSN 1744-683X

RSC Publishing

PAPER

Zhenkun Zhang and Eric Grelet

Tuning chirality in the self-assembly of rod-like viruses by chemical surface modifications

1744-683X(2013)9:4;1-H

Soft Matter

RSC Publishing

PAPER

Tuning chirality in the self-assembly of rod-like viruses by chemical surface modifications†

Cite this: *Soft Matter*, 2013, **9**, 1015

Zhenkun Zhang‡ and Eric Grelet*

Filamentous viruses of similar molecular and subunitary structure can form either a liquid crystalline nematic phase or a chiral nematic – also called cholesteric – phase, which is an elegant example of how self-organization of nanorods, with otherwise similar properties, can be affected by only subtle differences of surface properties and of the arrangement of the constituent subunits. In this work, we studied the influence of viral surface properties on the self-assembly of rod-like *fd* virus suspensions into the chiral nematic phase. For this purpose, the filamentous *fd* virus has been subjected to various chemical modifications on its capsid proteins: several organic molecules of different sizes and structures, including two popular fluorescent dyes (fluorescein and rhodamine), were coupled to the surface amino groups of the virus. The resulting chemically modified viruses still form a cholesteric phase in an aqueous suspension, but with a lower helicity compared to suspensions made of wild-type *fd* viruses. The degree of unwinding of the helical periodicity (or cholesteric pitch) depends on the structure of the labeled molecules. In addition, the chemically modified viruses exhibit a well-defined first order phase transition between the isotropic liquid and the liquid-crystalline state. Besides these modifications targeting the amino groups, the surface carboxyl groups were coupled with amino compounds so that the surface charge of *fd* viruses was reversed from negative to positive. The resulting particles can only form a nematic phase without any macroscopic helicity. These results suggest that inter-particle interactions, together with the intrinsic chirality of the virus, play an important role in the origin of the helical twist in the cholesteric phase.

Received 1st October 2012
Accepted 8th November 2012

DOI: 10.1039/c2sm27264d

www.rsc.org/softmatter

Introduction

Filamentous viruses, such as *fd*, M13 and TMV, have attracted tremendous interest. Some of them are platforms for the phage display technique from which drugs and antibodies can be cultivated,[1] and building blocks for functional materials of potential applications.[2–6] In addition, these viruses have been used as model colloidal rods due to their high monodispersity, tunable flexibility and well-defined surface properties.[7,8] As a typical example of the latter aspect, the lyotropic liquid crystalline phases formed by the rod-like *fd* virus have been investigated intensively in recent years.[8–16] By increasing the *fd* virus concentration, the first mesophase following the isotropic liquid phase is the chiral nematic or cholesteric phase in which the average particle orientation (also called the director) rotates helically along a given axis.[10] As a consequence of the twisted structure, well-defined optical "fingerprint" textures related to the cholesteric periodicity or pitch are observed under a polarizing optical microscope. Many efforts have been dedicated to understanding the origin of the helical feature of this cholesteric phase, stimulated by the fact that some other filamentous viruses with very similar structure, such as pf1 or TMV, only form a pure nematic phase without any twist between the mesogens.[11,14,15] The distinct nature of the liquid crystalline phase formed by these rod-like viruses with very similar molecular structures is a significant example of how tiny differences in microscopic surface properties can influence the self-assembly behavior of colloidal particles.[17] Manipulating the surface properties and therefore the inter-particle interactions to tune the self-organization and the helicity of the cholesteric phase constitutes an appealing step to determine which parameters control the helical twist of the chiral nematic phase. For this purpose, we have performed in this work several chemical modifications on the rod-like *fd* virus and we have investigated the influence of such modifications on the phase behavior of the virus suspensions. Knowledge learned from this work might be useful for manipulating the self-assemblies of virus based building blocks, a field emerging recently.[18–21]

Université de Bordeaux et CNRS, Centre de Recherche Paul-Pascal, 115 Avenue Schweitzer, F-33600 Pessac, France. E-mail: grelet@crpp-bordeaux.cnrs.fr

† Electronic supplementary information (ESI) available: Mass spectrometry of the *fd* virus modified with methyl acetimidate (*fd*-MA), UV-visible spectra of *fd* viruses labeled with dyes and determination of A269/A491 for pure FITC. See DOI: 10.1039/c2sm27264d

‡ Present address: Key Laboratory of Functional Polymer Materials, Ministry of Education, Institute of Polymer Chemistry, Nankai University, Tianjin 300071, P. R. China.

Fd virus is a rod-like particle consisting of a circular single stranded DNA surrounded by a protein capsid.[22] The protein capsid contains around 2700 identical major coat proteins, g8p, which are helicoidally wrapped following a five-fold rotation axis combined with a two-fold screw axis.[22] Each g8p is composed of about 50 amino acid residues and has a α-helix conformation. Opportunities for chemical modifications are offered by the abundant amino and carboxyl groups on the g8p coat protein, especially at the solvent-exposed N-terminal part.[23–26] The agents we chose for the chemical modifications of the surface amino groups are methyl acetimidate (MA) and two common fluorescent dyes: fluorescein isothiocyanate (FITC) and *N*-hydroxysuccinimide (NHS) esters of 5-(6)-carboxy-X-rhodamine (ROX) (Scheme 1). These chemicals represent different sizes, structures and functionalities applied on the virus surface. In particular, the availability and low cost of the two popular dyes (FITC and ROX) allow a systematic study of the phase behaviors of dye-labeled viruses on their own. Such studies are relevant to tracer and tracking techniques for which a few fluorescent dye-labeled particles are dispersed in the background of the unlabeled parent particles.[27–29] An implicit assumption is that the labeled particles behave similar to the unlabeled ones. In this work, we intend to address whether or not this assumption is valid.

Besides the modifications which target the amino groups, we have previously reported a method to reverse the surface charge of the *fd* virus from negative to positive by permanently modifying the carboxyl groups with amines after carbodiimide activation (Scheme 1C).[25] The liquid crystalline phase behavior of these charge-reversed viruses, as well as of the above amino-targeting modified viruses, is also fully characterized in this work.

This paper is organized as follows: some general physico-chemical features (number of modified surface groups, charge properties, *etc.*) of the modified viruses are first investigated. Then we determine the isotropic–(chiral) nematic (I–$N^{(*)}$) phase transition as well as the quantitative helicity of the liquid crystalline cholesteric phase. These properties are compared with those of the unmodified viruses under the same experimental conditions in terms of pH, ionic strength, and temperature. Finally, we discuss the different mechanisms of chirality amplification in the liquid crystalline organization of chiral colloidal rods.

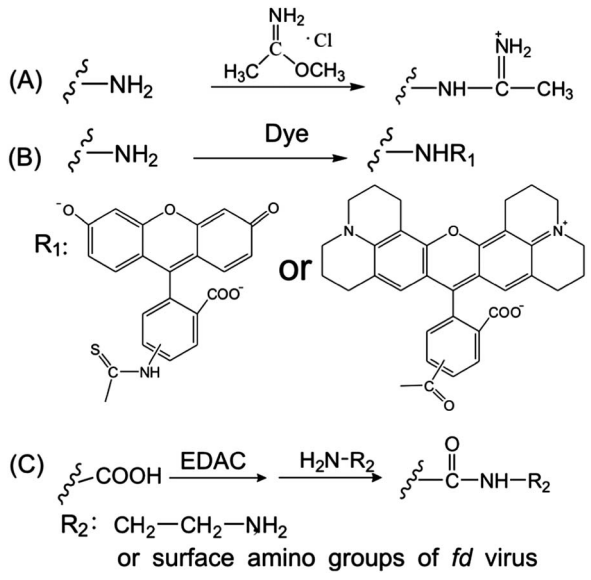

Scheme 1 Chemical modifications of the surface amino groups and carboxyl groups of the *fd* virus coat proteins performed in the present study. (A) Amino groups are coupled with methyl acetimidate (MA). (B) Amino groups are labeled with fluorescein isothiocyanate (FITC) or succinimidyl ester of 5-(6)-carboxy-X-rhodamine (ROX). (C) Carboxyl groups of the amino acids Glu2, Asp4, Asp5, Asp12 or Glu20 can be modified with different organic amines, such as ethylenediamine (EDA), after being activated by 1-ethyl-3-(3-dimethylaminopropyl) carbodiimide hydrochloride (EDAC).

Experimental results

Materials

Fluorescein isothiocyanate (FITC), succinimidyl ester of 5-(6)-carboxy-X-rhodamine, (ROX), 1-ethyl-3-(3-dimethylaminopropyl)carbodiimide hydrochloride (EDAC), methyl acetimidate (MA) and ethylenediamine dihydrochloride (EDA) were obtained from Sigma-Aldrich and used without further purification. Other solvents and agents are in the highest purity available commercially. Water from a Millipore Milli-Q10 system (>18.2 MΩ) was used. The aqueous buffer mentioned in the work is a single batch of TRIS–HCl buffer (20 mM TRIS, pH 8.2), the total ionic strength (I = 15 mM) being adjusted by adding 5 mM of NaCl (20 mM TRIS corresponds to I = 10 mM at pH = pK_a ~ 8.2 at room temperature). *Fd* viruses were grown and purified following standard biochemical protocols using the XL-1 blue strain of *E. coli* as the host bacteria.[30]

Surface modifications

(1) FITC and ROX labelling. To a *fd* virus suspension at 10 mg mL^{-1} in 100 mM phosphate buffer (pH 8.0), FITC or ROX in DMSO was added dropwise. The molar ratio of the dye to each coat protein was controlled at 5 : 1 in order to achieve maximum labelling efficiency. The volume fraction of DMSO in the final mixture was not more than 10% to avoid damage to the virus. The resulting mixtures of dyes and viruses were kept ready overnight in the dark. Free dyes were removed by intensive dialysis steps, first against distilled water and then against the TRIS–HCl–NaCl buffer at I = 15 mM. The dialyzed viruses were further ultra-centrifuged (200 000*g* for 3 hours) and redispersed in the desired buffer three times. Within the sensitivity of our instrument, no absorption can be detected in the supernatant of the last round of ultra-centrifugation at the characteristic absorption wavelength of each dye, meaning that the unbound dyes were removed as much as possible. Hereafter *fd* viruses labelled with FITC or ROX are referred to as *fd*-FITC and *fd*-ROX, respectively.

(2) Modification of the *fd* virus with methyl acetimidate (MA). The procedure described by Armstrong *et al.*[31] was applied. *Fd* viruses were dispersed into 100 mM sodium borate buffer (pH 9.0) to form a suspension at 5 mg mL^{-1} of viruses. 5 mL of the suspension was then cooled down to about 0 °C in an ice-water bath, to which 55 mg of MA was added. After 30 min, the ice-water bath was removed and the reaction

mixture was dialyzed first against distilled water and then against the chosen buffer. The as-modified virus will be referred to as *fd*-MA in the following text.

(3) Charge reversal of *fd* viruses. The detailed procedure of the charge reversal of *fd* viruses by carbodiimide chemistry has been published elsewhere.[25] An optimized procedure is briefly summarized here. A solution containing 200 mM ethylenediamine dihydrochloride (EDA) was prepared and the pH was adjusted to 5 by adding diluted NaOH solution. Then, 4.5 mL of EDA solution was mixed with 0.5 mL of an *fd* virus stock suspension at 20 mg mL^{-1} virus. The final pH of the resulting suspension was kept between 5 and 5.5. To this suspension, 1 mole of EDAC was added. The reaction was allowed to proceed at room temperature for 5 hours and then the same amount of EDAC was added again. The final dispersion was dialyzed against distilled water to remove residual amines and other by-products. The dialyzed dispersion was further centrifuged at 12 000*g* to remove potential inter-virus cross-linked *fd* viruses, if any. The charge reversed *fd* virus will be referred to as *fd*-EDA.

Concentration determination of the (chemically modified) viruses

The wild-type *fd* virus exhibits a characteristic absorption peak at 269 nm, which can be used to determine the virus concentration in aqueous solution with an extinction coefficient of 3.84 cm^2 mg^{-1} at this wavelength.[32] The virus modified with MA (*fd*-MA) and the charge reversed one (*fd*-EDA) display the same absorption behavior as the wild-type *fd* virus in the near-UV range (results not shown). It is therefore assumed here that the same extinction coefficient can be used to determine the concentration of these chemically modified viruses. However, special care is needed when determining the concentration of viruses labeled with dyes. Indeed, both FITC and ROX moieties show a residual absorption at 269 nm, besides their characteristic absorption peak at longer wavelength (Fig. S2 in the ESI†). At a well-defined pH value of 8.2, the maximum in the absorption spectrum of FITC and ROX is located at 491 nm and 583 nm, respectively. The ratio, a, of the absorption of free dyes at 269 nm over the characteristic maximum absorption was determined and used to calculate the real concentration, C_{real} (mg mL^{-1}), of the suspension of dye labeled viruses by the following relationship:

$$C_{real} = \frac{(A_{269} - B) - (A_{dye} - B) \times a}{3.84} \times b \quad (1)$$

here, A_{269} is the absorption of the dye labeled viruses at 269 nm, which includes contributions from both the dyes and the viruses, A_{dye} is the absorption of the dye labeled viruses at the characteristic absorption wavelength of each dye (which is in the visible range where the *fd* virus has no absorption), b is the dilution factor, and B is the baseline of the corresponding buffer. The value of a for *fd*-FITC and *fd*-ROX is 0.35 and 0.58, respectively (see ESI†).

The amount of dyes labeled onto each virus (N_{dye}) can then be determined by:

$$N_{dye} = \frac{(A_{dye} - B)}{\varepsilon' \times C_{real}} \times M_{fd} \times b \quad (2)$$

where A_{dye}, B, C_{real}, and b are the same parameters as those in eqn (1), M_{fd} is the molecular weight of *fd* virus (1.64×10^7 g mol^{-1}), and ε' is the molar extinction coefficient of each dye. Under the conditions of this work, $\varepsilon' = 68\,000$ and $79\,000$ M^{-1} cm^{-1} for FITC and ROX, respectively.[33] The results are given in Table 1.

SDS-PAGE, agarose gel electrophoresis (AGE) and apparent zeta potential

(1) SDS-PAGE was performed following the standard Laemmli method.[34] A gel with a density of 18% was used. Wild-type or modified *fd* viruses were denatured in a buffer containing 1.6% SDS, 1% β-mercaptoethanol, 12.5% glycerol, 0.0025% bromophenol blue and 50 mM TRIS–HCl buffer (pH 7.6) (final concentrations). The gel was run under a buffer condition of 1% SDS, 1.92 mM glycine, 250 mM TRIS (final concentrations). Gels were stained with Coomassie Brilliant Blue R-250 for visualizing the protein bands.

(2) Agarose gel electrophoresis of non-denatured (modified) *fd* viruses was run on a 1% agarose gel following the procedure devised by Griess *et al.*[35] Suspensions of the (modified) *fd* viruses (10 μL, 0.1 mg mL^{-1} in 2 mM TRIS–HCl buffer) were combined with an aqueous solution of bromophenol blue (2 μL, 2.5 mg mL^{-1}) and loaded into the sample wells. The gel was run in 1× TAE buffer with an applied electric field 1 V cm^{-1} for 12 hours. The gel was stained in an aqueous buffer containing 0.5 g L^{-1} Coomassie blue G250, 25% 2-propanol and 10% acetic acid for 3 hours and finally destained in 10% acetic acid solution (v/v) for several days.

(3) The apparent electrophoretic zeta potentials of viruses were determined using laser Doppler electrophoresis on a Zetasizer 2000 equipped with an aqueous dip cell (Malvern, England). Viruses with or without chemical modifications were dispersed in 2 mM TRIS–HCl buffer (pH 8.2) to form 0.1 mg mL^{-1} suspensions. The average electrophoretic mobility from thirty measurements was converted to the zeta potential, using the Smoluchowski formula ($\xi = 4\pi\eta\mu/\varepsilon$, where μ, η and ε are the mobility of the particle, the viscosity and the dielectric constant of the dispersion, respectively).

Isotropic–(chiral) nematic phase transition

All (chemically modified) viruses were purified and dispersed in TRIS–HCl–NaCl buffer (pH 8.2, $I = 15$ mM), which was prepared in a single batch of 6L for a better comparison and reproducibility of the results. The concentrated virus suspensions were diluted to the coexistence region between the isotropic liquid and the (chiral) nematic phases (*I–N* phase transition) and left until macroscopic phase separation occurred. The lower part of the sample exhibiting birefringence corresponds to the (chiral) nematic phase of higher density, while the upper part of the sample is the isotropic liquid phase. Small portions of each phase were carefully pipetted from the sample while observing through crossed polarizers in order to avoid mixing of the two

Table 1 General properties of the chemically modified *fd* viruses

Name	Modification (targeting groups)[a]	No. of coupled agents per virus	I/N^b (mg mL^{-1})	ζ^d (mV)	$-\nu^e (P_0 \propto c^{\nu})$
wt-*fd*	—	—	14.2/16.0	−30.0	1.53
fd-MA	MA(–NH_2)	>2700 (ref. 31)	14.5/15.7	−28.0	1.77
fd-FITC	FITC(–NH_2)	*Ca.* 1360	14.5/16.9	−39.0	1.47
fd-ROX	ROX(–NH_2)	*Ca.* 1120	16.1[c]	−38.0	1.45
fd-EDA	EDAC + EDA(–COOH)	—	20.1 ± 1.3[c]	+21.5	—

[a] MA: methyl acetimidate; FITC: fluorescein isothiocyanate; EDAC: 1-ethyl-3-(3-dimethylaminopropyl) carbodiimide hydrochloride; EDA: ethylenediamine; ROX: 5-(6)-carboxy-X-rhodamine, succinimidyl ester. [b] The two values correspond to the virus concentration in the isotropic (I) and (chiral) nematic phase ($N^{(*)}$), respectively, at the I–N phase transition. [c] Concentration measured in a sample containing both isotropic liquid and nematic domains. [d] Apparent zeta potentials. [e] Slope, ν, obtained by fitting with a power law the cholesteric pitch, P_0, as a function of the virus concentration.

phases. The virus concentration in each phase was determined by the above mentioned UV spectrophotometrical method. For *fd*-ROX, the strong red/violet color makes difficult the visualization of the phase separation. In this case, a highly concentrated suspension was diluted to the coexistence region at the I–N transition. The concentration was measured in such a sample and was taken as the phase transition concentration. In the case of *fd*-EDA, gelation-like behavior occurs before full phase separation, and therefore the same procedure as described above for *fd*-ROX has been applied to determine the I–N transition.

Self-organization of the (chiral) nematic phase

Highly concentrated virus stock suspensions were prepared, close to the nematic to smectic phase transition. Sequential dilution of the stock suspensions resulted in a set of samples of varying concentration, spanning the whole nematic phase, which were filled into 1.5 mm quartz capillary tubes (sealed with flame). The samples in the capillary tubes were equilibrated for at least three days, and were then observed by polarizing optical microscopy to monitor the structure of the (chiral) nematic phase. The optical "fingerprint" textures characteristic of the cholesteric phase were recorded with a CCD camera (JAI, CV-M7) and analyzed with the software ImageJ. The distance between two bright and two dark lines corresponds to the cholesteric pitch, P_0. For a given sample, the reported P_0 value is an average of about twenty measurements sampling the different areas along the whole capillary tube. Note that a few labeled viruses *fd*-ROX have been added to *fd*-FITC suspensions (with a ratio of $1/10^5$) in order to determine by fluorescence microscopy the handedness of the cholesteric phase formed by *fd*-FITC modified viruses.[9] However, we were not able to visualize the guest *fd*-ROX particles in the cholesteric host of *fd*-FITC due to some overlap of the absorption/emission spectra of the two dyes (Fig. S2 in the ESI†), making difficult the handedness determination.

Results and discussion

General properties of the modified viruses

Four kinds of chemical modifications were applied to the *fd* virus, targeting different functional groups of the viral surface. Table 1 summarizes the main physicochemical properties of the modified viruses. MA is a small molecule which reacts with the amino groups of the g8p of the *fd* virus, converting the surface amino groups into amides.[31] The modification with MA results in complete blocking of all of the surface amino groups, as confirmed by Armstrong *et al.* and also by MALDI-TOF in this work (see Fig. S1 in the ESI†).[31] In this case, the charge property of the *fd* virus does not change. Compared to MA, FITC and ROX are much larger molecules exhibiting an aromatic structure. ROX, a derivative of rhodamine, has a propensity to form dimers (Scheme 1B).[36–39] More than one thousand dye molecules were chemically bound to each virus (Table 1), which is comparable to the values reported by others when labelling similar dyes to filamentous viruses.[23,24] In addition, a much more complicated modification was implemented by first activating the surface carboxyl groups and then reacting with amino compounds (EDA). The total effect of this modification is the charge reversal of the virus from negative to positive (*fd*-EDA) as revealed by electrophoresis and by zeta potential measurements (Table 1).

The coat proteins, g8p, of the (modified) viruses were analyzed by SDS-PAGE (Fig. 1A). The g8p of viruses modified by MA, FITC or ROX appears as a single band which has the same migration distance as that of the wild-type *fd*. The gel is not sensitive enough to resolve the molecular weight difference introduced by one or two coupled organic compounds. But these results at least indicate that no dramatic changes such as degradation or cross-linking of the coat proteins occur during the chemical modification. For *fd*-EDA, multiple bands were observed, which correspond to singlet, dimer, trimer, *etc.*, of the coat protein. This is due to cross-linking of g8p as discussed in a previous work.[25] This cross-linking occurs because both the amino groups of the virus itself and the free amino compounds in the solution can react with the activated carboxyl groups after the activation step (Scheme 1C). If the amino groups react with the activated carboxyl groups on the same coat protein, intra-protein cross-linking can be formed (illustrated by the dashed lines with double arrows in Fig. 1D). The cross-linking between adjacent coat proteins results in inter-protein cross-linking of two or more coat proteins corresponding to the different bands in Fig. 1A, and represented by the solid lines with double arrows in Fig. 1D. Both kinds of cross-linking consume one amino group and carboxyl group while introducing two or four

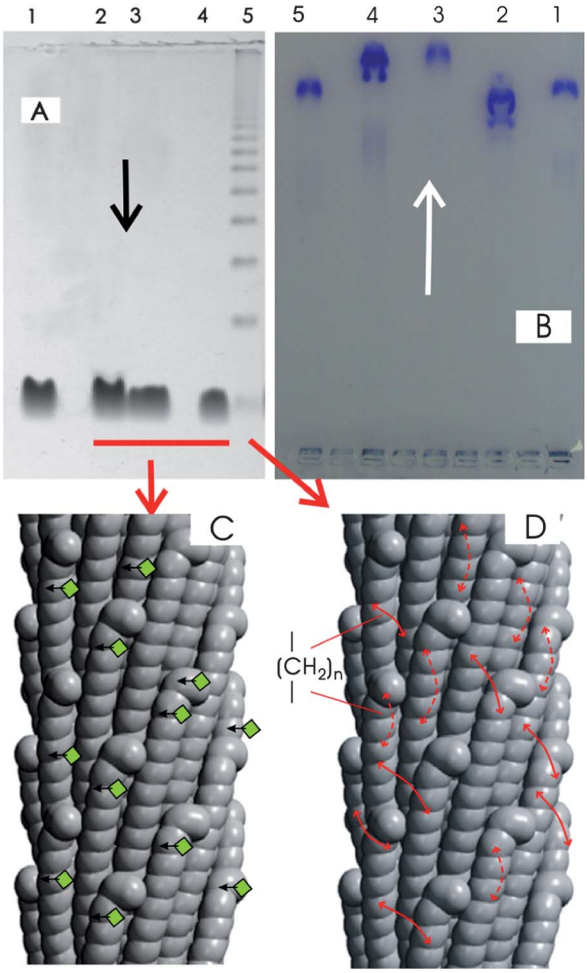

Fig. 1 (A) SDS-PAGE of the coat protein, g8p of the (chemically modified) *fd* viruses. Lane 1: wild-type *fd*; lane 2: *fd*-MA; lane 3: *fd*-FITC; lane 4: *fd*-ROX; lane 5: *fd*-EDA. (B) Agarose gel electrophoresis of viruses. Lane 1: wild-type *fd*; lane 2: *fd* Y21M; lane 3: *fd*-MA; lane 4: *fd*-FITC; lane 5: *fd*-ROX. The arrow in (A) and (B) indicates the electrophoretic direction. (C) and (D) Schematic illustrations of the surface of the *fd* virus after chemical modifications. (C) *Fd* modified with MA, FITC or ROX represented by the green diamonds on the virus surface. (D) *fd*-EDA. The dashed and solid double arrow lines represent intra-protein and inter-protein cross-linking, respectively (see text).

hydrophobic methylene groups. By this way, loop-like structures containing hydrophobic segments are introduced onto the surface of the virus (Fig. 1D). As a consequence of the cross-linking, it is expected that the regular helical arrangement of the solvent exposed part of the g8p coat protein on the virus surface is disrupted. It has been shown that MA mainly binds to the amino groups of Lys8 of the N-terminal part if the incubating time is short, while modifications of amino groups in the C-terminal part can occur only after long-time exposure of the *fd* virus to MA.[31] However, we found by CNBr denaturation and the MALDI-TOF mass spectroscopy technique that the modifications of the C-terminal also occur even in the case of short incubating time, and double modifications of Ala1 and Lys8 are the common case (see Fig. S1 in the ESI†).

The coat protein, g8p, in the protein capsid of the virus can be roughly divided into the C-terminal part which interacts with the viral DNA and the N-terminal part, which is exposed to the solvent. Both parts contain reactive functional groups which are *a priori* available for chemical modifications. In the case of dye labeling, Li *et al.* have recently shown that the labeling of rod-like viruses with fluorescent dyes such as rhodamine mainly occurs to the amino groups of Ala1 and Lys8 of the coat proteins in the N-terminal part.[23] In the case of *fd* modified with EDA by carbodiimide chemistry, we have shown in our previous work that only the surface carboxyl and amino groups take part in the reactions.[25]

The (modified) viruses were subjected to non-denatured agarose gel electrophoresis (AGE) (Fig. 1B).[35] *Fd*-MA, *fd*-FITC and *fd*-ROX migrate as a single band, just like the wild-type *fd*, suggesting integrity of the virus structure and homogeneity of the chemical modifications. The migration distances of wild-type *fd* and *fd*-ROX are identical and slightly less than those of *fd*-MA and *fd*-FITC (Fig. 2B). In addition, the zeta potentials for the modified viruses are very similar within experimental uncertainty (Table 1). All these results indicate that the modified viruses (except *fd*-EDA) exhibit very close surface charge properties. In contrast to the amine-modified viruses, the positively charged *fd*-EDA stays in the loading well of the gel without moving. This behavior was also observed with other positively charged virus particles and was attributed to adherence of the particles to the gel matrix.[40] Nevertheless, the rod-like shape and the structural integrity of *fd*-EDA have been confirmed previously by transmission electron microscopy.[25]

Similar to the wild-type *fd* virus, suspensions of *fd*-MA, *fd*-ROX or *fd*-FITC exhibit a macroscopic phase separation at the *I*–*N* phase transition. For wt-*fd*, the results of the virus concentrations including the absolute concentration values and the coexistence phase range are in good agreement with previous measurements under the same conditions.[10,12,13,15] In the case of chemically modified viruses, *fd*-MA has the same phase coexistence range as wild-type *fd* within experiment error, while the

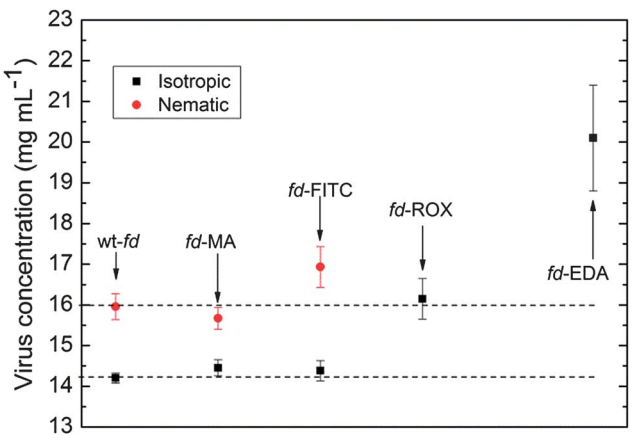

Fig. 2 Virus concentrations at the isotropic liquid and (chiral) nematic phase transition (*I*–*N*). The ionic strength is 15 mM (TRIS–HCl–NaCl buffer, pH 8.2). In the case of wild-type *fd*, *fd*-MA and *fd*-FITC, the concentrations of the isotropic and nematic phases were determined after macroscopic phase separation. For *fd*-ROX and *fd*-EDA, the concentration refers to samples exhibiting the coexisting isotropic liquid and nematic phases. The dashed lines represent guides for the eyes.

phase coexistence range of *fd*-FITC is slightly wider than the one of wt-*fd*. This difference might be due to the uncertainty in the concentration determination of the fluorescent dye labeled viruses.

For *fd*-ROX, the concentration reported here is the value below which only the isotropic liquid phase containing some nematic domains can be observed by polarizing optical microscopy after sequential dilution from a concentrated stock (see above). This value is located between the coexisting phase range of both wild-type *fd* and *fd*-FITC, suggesting that *fd*-ROX has a coexisting phase range comparable to these two virus suspensions. In the case of the positively charged *fd*-EDA, a suspension of *fd*-EDA which is very close to the phase boundary and containing several nematic domains became turbid but did not undergo a macroscopic phase separation, since finally the turbid suspension turns into a non-flowing gel-like state. This gelation only occurs for concentrated suspensions, while diluted samples of only several mg mL^{-1} can be stable in a sol state for a long time when stored at 4 °C. The reasons for this gelation might be the hydrophobic attractions between the modified viruses. Since the modification procedure introduces hydrophobic loops onto the virus surface which can induce attractive interactions between the rod-like particles in aqueous solution (see Fig. 1D), we mention here that another filamentous virus, the phage X, with hydrophobic motifs on its surface also forms a gel-like structure in a suspension rather than a flowing nematic phase.[11]

Self-organization of the chiral nematic phase

The details of the self-organization of the (chiral) nematic phase formed by the chemically modified viruses have been investigated by polarizing optical microscopy (Fig. 3 and 4). Cholesteric fingerprint textures are seen in the suspensions of *fd*-FITC and *fd*-ROX after equilibrium for a few days (Fig. 3B and C), just like the wild-type *fd* virus (Fig. 3A). Parallel dark and bright stripes developed homogeneously along the wall of the capillary, corresponding to particles normal and parallel to the sample plane, when observed at 45° of crossed polarizers, respectively. In contrast, there is no visible cholesteric pattern in the charge-reversed *fd*-EDA suspensions, except some birefringence attributed to nematic order (Fig. 3D).

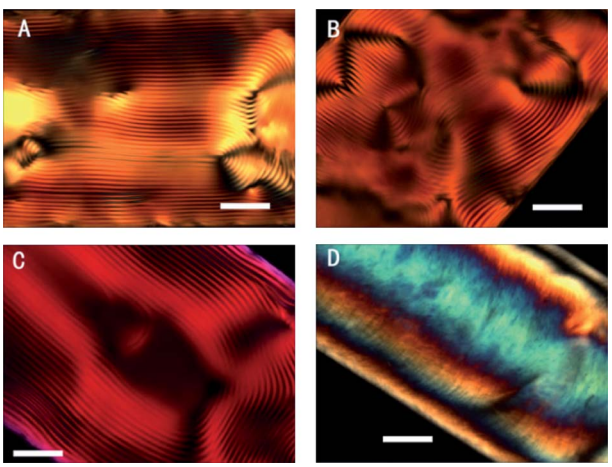

Fig. 3 Typical optical texture of (chemically modified) *fd* virus suspensions observed by polarizing microscopy. The scale bars indicate 300 μm. For all samples, the ionic strength is 15 mM (TRIS–HCl–NaCl buffer, pH 8.2). (A) Wild-type *fd*, $C = 39.5$ mg mL^{-1}. (B) *fd*-FITC, $C = 33.6$ mg mL^{-1}. (C) *fd*-ROX, $C = 42.5$ mg mL^{-1}. (D) *fd*-EDA. $C = 33.8$ mg mL^{-1}.

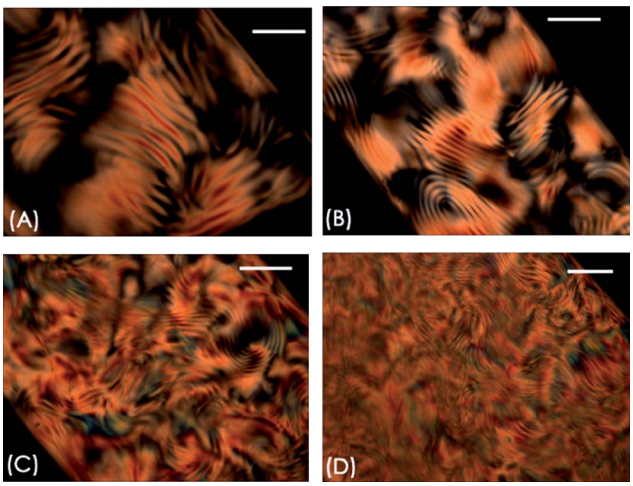

Fig. 4 Cholesteric textures of the *fd* virus modified with methyl acetimidate (*fd*-MA) at different concentrations. The scale bars indicate 300 μm. The ionic strength is 15 mM (TRIS–HCl–NaCl buffer, pH 8.2). (A) 25.4 mg mL^{-1}. (B) 36.0 mg mL^{-1}. (C) 45.8 mg mL^{-1}. (D) 54.5 mg mL^{-1}.

In the case of *fd*-MA, much more complicated microstructures are observed (Fig. 4). Domains with regular cholesteric fingerprints but with different orientations appear in the sample at low concentration (Fig. 4A and B). At higher concentration, small cholesteric domains coexist with areas showing less ordered structure with typical features ranging from inter-winded thread-like stripes to randomized fingerprints (Fig. 4C and D). The homogeneity and the degree of ordering of the patterns become worse with increasing virus concentration while, for wild-type *fd*, *fd*-FITC and *fd*-ROX, more regular fingerprint structures usually exist deep in the cholesteric range. The abnormality of *fd*-MA was first attributed to kinetics, the samples requiring time to reach their equilibrium state, but inspection after three months revealed no significant evolution.

The cholesteric phase of the (modified) viruses was mainly characterized by the absolute value of the twist periodicity, also called the pitch P_0, which is a function of virus concentration as summarized in Fig. 5. For *fd*-MA the pitch was only measured in the domains with regular fingerprint and values from different domains are close enough to determine an average value (Fig. 4). The data were fitted with a power law ($P_0 \propto c^{\nu}$), and the resulting values of ν are listed in Table 1. The properties of the cholesteric phases of the (modified) viruses are different from each other. If the exponent ν does not significantly vary between the different virus systems, it turns out that with identical conditions in terms of temperature, pH and ionic strength, all modified viruses have, at a given concentration, a larger pitch than wild-type *fd* (Fig. 5), with the following order by decreasing pitch magnitude: *fd*-ROX > *fd*-MA > *fd*-FITC > wt-*fd*.

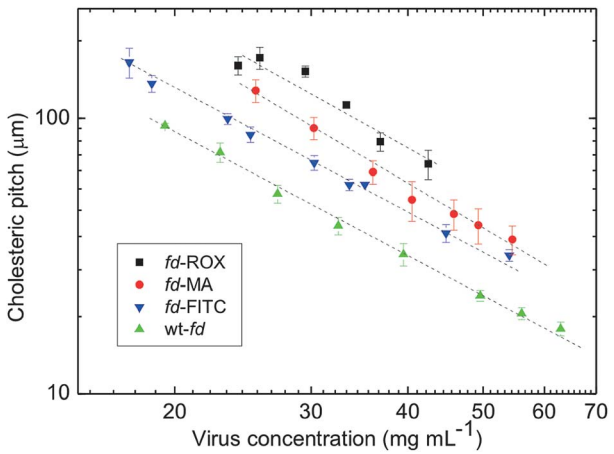

Fig. 5 Log–log plot of the cholesteric pitch (P_0) as a function of concentration (C) for the different chemically modified viruses. The ionic strength is 15 mM (TRIS–HCl–NaCl buffer, pH 8.2). In the case of *fd*-ROX and *fd*-FITC, the concentrations are calibrated by subtracting the absorbance contribution of the corresponding dye at 269 nm. Data were fitted according to a power law relationship $P_0 \propto c^{\nu}$. The resulting values of ν are listed in Table 1.

Discussion

Fd virus consists of about 2700 α-helical coat proteins which are helicoidally wrapped around the inner DNA, making this filamentous virus an intrinsic chiral particle. The connection between molecular chirality and macroscopic helicity as exhibited in the cholesteric phase remains an unsolved question, despite recent works shedding new light on this fundamental problem.[9,11,14,41–43] For instance, we have shown in a previous work that *fd* viruses grafted with a neutral and achiral polymer–poly(ethylene glycol) (PEG) still form a cholesteric phase, although the intrinsic chiral nature of the virus is expected to be fully screened by the polymer layer.[15] Whereas the *fd* virus grafted with neutral PEG forms a cholesteric phase,[15] we observed that the *fd* virus grafted with a thermosensitive polymer, poly(*N*-isopropylacrylamide) (PNIPAM), tends to form only a nematic phase, especially at high ionic strength and concentration where inter-particle interactions are dominated by the polymer layer.[44] These results indicate that the surface properties, regardless of any additional mechanism, play an important role in the formation of the cholesteric phase.

Based on a large body of work, Tomar *et al.* claimed that one can tune the nature of the (chiral) nematic phase of several filamentous viruses, including *fd*, by using dopants such as surfactants and metal ions which can specifically bind to the viral DNA or the coat protein.[11] More recently, Barry *et al.* found that the cholesteric phase of a mutant of *fd* virus, *fd* Y21M, has a handedness opposite to the wild-type one, although the only difference between these two viruses is that tyrosine (Y) at the position 21 of each coat protein in the wild-type is replaced by methionine (M) in the mutant. Moreover, the cholesteric pitch of this mutant is larger than the wild-type one under identical conditions.[14] The authors of the two works interpreted their results in the framework of the following hypothesis: the *fd* virus adopts in an aqueous suspension a dynamical "cork-screw" shape or a supramolecular helical conformation[15] which is assumed to stem from the incommensurate interaction between the viral DNA and the coat proteins.[11] This mesoscopic length-scale chirality would be responsible for the macroscopic twist of the cholesteric phase. This scenario is supported by a recent report where a chiral filamentous virus, M13, a close mimic of the *fd* virus, seems to exhibit a rough helical contour shape with a pitch 290 nm after being chemically trapped in a polymeric gel.[45]

Alternatively, an electrostatic based model supported by experiments and proposed by Tombolato *et al.* points out that the steric helical arrangement of the coat proteins and the resulting helical distribution of surface charges on the virus can promote twist with opposite handedness. The balance between the steric and the electrostatic contributions is very sensitive to the details of each particle structure, and more specifically to the location of the charges on the virus surface. This strong dependence of the viral capsid symmetry might then explain the diversity of the chiral self-assembly behaviors when biological particles are self-organized into liquid-crystalline phases.[9,42,46]

In this work, *fd* virus was subjected to different kinds of chemical modifications in order to tune the helicity of the virus in its cholesteric phase. The resulting viruses can be classified into three types: (1) viruses modified with the small molecule-MA. This modification converts surface amino groups into amides while keeping *a priori* unchanged the charge properties of the viruses and at the same time introducing an extra methyl group.[31] (2) Viruses modified with the dyes-FTIC or ROX. During the dye labeling, parts of the coat proteins are coupled with the dye moieties. The resulting virus can be seen as a "hybrid" consisting of chemically modified coat proteins in coexistence with intact coat proteins. Indeed, less than half of the coat proteins per virus are labeled (Table 1). (3) Charge reversed viruses (*fd*-EDA), where both the surface amino and carboxyl groups take part in the reaction. Some of the coat protein subunits are then chemically cross-linked, introducing hydrophobic loops onto the virus surface. By this way, the regular surface of the virus may be deliberately altered, changing therefore its liquid crystal phase behavior.

The viruses modified with MA, FITC and ROX have similar *I*–*N* phase transition with respect to the wild-type one (Table 1 and Fig. 2). In addition, just like the wild-type *fd* virus, all of the modified viruses, except charge-reversed *fd*-EDA, form a cholesteric phase. Under the same conditions, the pitch of all modified viruses is larger than the wt-*fd* one (in the case of positively charged *fd*-EDA, the nematic phase can be seen as a cholesteric one with an infinite pitch) (Fig. 2–5).

The *I*–*N* transition and phase coexistence range of rod-like particles depend mainly on three rod features, which are aspect ratio, flexibility, and surface charge density.[12,14] As previously mentioned, Barry *et al.* observed that the mutant *fd* Y21M has lower concentrations of coexisting isotropic liquid and chiral nematic phases and a wider coexistence range than the wild-type *fd*,[14] while both viruses have very similar surface charge and aspect ratio (Fig. 1).[8] This result is a direct consequence of the higher stiffness of the former, exhibiting a persistence length 3.5 times larger than the latter.[14] In contrast to the *fd* Y21M and

fd phages, similar phase transition behavior between the wild-type virus and the modified ones with MA, FITC and ROX indicates that the chemically modified and the wild-type viruses exhibit comparable flexibility since gel electrophoresis experiments have shown no significant change in the surface charge property (Table 1 and Fig. 1B). Moreover, the persistence length of the *fd* virus labeled with Alexa 488, a dye similar to FITC used in this work, is similar within the error bars to the wild-type one.[14,47] Even in the extreme case of a charge reversed virus which involves cross-linking between the surface amino and carboxyl groups, dynamic light scattering hints that the stiffness of *fd*-EDA is only slightly different from the wild-type.[25]

However, we cannot exclude the possibility that the coat proteins of the capsid of the modified viruses exhibit a different helical symmetry compared to the native one, *i.e.* the chemical modifications may promote some rearrangement of the coat proteins that would influence the conformation of the virus. However, our modifications occur to the solvent exposed N-terminal part of the coat protein (from position 1 to 20, roughly). In the long journey of elucidating the structure of filamentous viruses, it has been demonstrated that manipulation of the N-terminal part by changing pH or temperature, by labeling with heavy atoms, or by point mutagenesis can affect the arrangement or the helical symmetry of the viral capsid, but only to a slight degree.[48–50] Indeed, the N-terminal part, where the current chemical modifications have been focused, has structurally a negligible importance since the last few amino groups can be removed without losing the structural integrity of the virus.[51–54] Thus the DNA–protein interaction may not be interrupted by our chemical modifications. In summary, if there is some change of the coat protein arrangement modified by the addition of our chemicals, this change is small enough not to significantly shift the rod flexibility of the chemically modified virus. Thus, keeping the flexibility similar, it is expected that our modifications may also not disturb the viral supramolecular helical conformation (if it does exist). Consequently, there should be other reasons that have to be invoked to account for the unwinding of the cholesteric pitch occurring in our modified viruses.

Although we have already mentioned that most of the modified viruses exhibit similar *average* surface charge density compared to the wild-type one (Table 1 and Fig. 1B), this does not necessarily mean that the corresponding helical charge distribution remains unchanged. Indeed, we have shown that the labeled viruses are only *partially* covered by the fluorescent dyes (Table 1 and Fig. 1), which implies that the helical charge distribution is *locally disturbed* by the fact that only about half of the coat proteins carry a chemical moiety. This yields local heterogeneities of the charge surface because the added molecules break the helical charge symmetry by their finite size and their steric hindrance. The resulting helical charge distribution is therefore altered and this breaking of the viral charge helical symmetry can decrease the intensity of the chiral interactions between viruses, inducing the partial unwinding of the cholesteric pitch of the modified viruses.

Finally, we speculate on a last contribution based on inter-particle interactions such as attractions brought by the chemical modifications which could play an important role in decreasing the cholesteric twist of the modified viruses. Indeed, FITC, ROX and MA moieties contain some hydrophobic part, due to the aromatic rings of the two dyes, and due to the methyl group of the MA molecule. Such hydrophobic interactions can induce some attractions between viruses when dispersed in aqueous solution.[55,56] The pitch of *fd*-ROX is larger than *fd*-FITC, which may be correlated with the higher hydrophobicity of ROX than FITC, so the former has stronger unwinding capacity than the latter. The *fd*-MA is worth being given more attention due to its pronounced difference compared to the wild-type *fd* virus in terms of the microstructure and pitch of the cholesteric phase (Fig. 4 and 5). Beyond the much larger pitch observed for *fd*-MA, the lack of homogeneity of the cholesteric pitch (Fig. 4C and D) is consistent with the presence of attractive interactions induced by the methyl groups. Such pitch behavior has already been observed for the *fd*-PNIPAM system when the grafted thermoresponsive polymer is hydrophobic at high temperature.[44]

In the case of *fd*-EDA, it is expected that the inter-protein cross-linking changes the helical symmetry of the virus surface by smearing out the steric and electrostatic bases of chirality amplification. In addition, the spontaneous gelation of the concentrated *fd*-EDA suspensions is a sign of (hydrophobic) attractions between rods for which a configuration based on parallel alignment could be favored (in contrast to electrostatic repulsive interaction, which favors twist between the rod-like particle to minimize the repulsion between charges).[12] Those factors together are responsible for the pure nematic phase observed with the charge-reversed virus suspensions. It is noted here that such an attractive interaction does not necessarily influence the macroscopic *I–N* transition, as previously shown by Dogic *et al.*, who observed that an effective attraction based on the depletion interaction has no effect on the *I–N* transition of an *fd* virus suspension at low ionic strength.[57]

Conclusions

In this work, chemical modifications were applied to the rod-like *fd* virus, aiming to tune its surface properties and to determine the influence of such changes on its phase behavior and chiral self-organized states. Different chemical compounds from small molecules to common dyes were introduced to the virus surface, with, in particular, the achievement of a charge-reversed virus. All the chemically modified virus suspensions exhibit a similar location of the isotropic–(chiral) nematic phase transition, but they differ from the wild-type one in terms of the helical pitch of the cholesteric phase. In the case of the charge-reversed viral particle, no macroscopic twist was observed, and only a nematic-like phase was formed. We show thus the importance of the N-terminal part of the coat protein in chirality amplification, and more specifically that disruptions of the helical symmetry of the viral capsid and hydrophobic interactions play a major role in controlling the macroscopic chiral behavior. Relevant to the tracer and tracking techniques, we can also conclude from our work that dye labeled particles behave essentially similarly to unlabeled ones, in terms of physical

features such as rod flexibility and thermodynamic bulk properties.

Acknowledgements

We would like to thank Johan Buitenhuis for his help in MALDI-TOF mass spectroscopy experiments, Pavlik Lettinga for fruitful discussions and the European network of excellence SoftComp for the financial support.

Notes and references

1 G. P. Smith and V. A. Petrenko, *Chem. Rev.*, 1997, **97**, 391–410.
2 B. Y. Lee, J. Zhang, C. Zueger, W.-J. Chung, S. Y. Yoo, E. Wang, J. Meyer, R. Ramesh and S.-W. Lee, *Nat. Nanotechnol.*, 2012, **7**, 351–356.
3 Y. J. Lee, H. Yi, W. J. Kim, K. Kang, D. S. Yun, M. S. Strano, G. Ceder and A. M. Belcher, *Science*, 2009, **324**, 1051–1055.
4 Y. Ma, R. J. M. Nolte and J. J. L. M. Cornelissen, *Adv. Drug Delivery Rev.*, 2012, **64**, 811–825.
5 C. Mao, A. Liu and B. Cao, *Angew. Chem., Int. Ed.*, 2009, **48**, 6790–6810.
6 Z. Zhang and J. Buitenhuis, *Small*, 2007, **3**, 424–428.
7 Z. Dogic and S. Fraden, in *Soft Matter-Complex Colloidal Suspensions*, ed. G. Gompper and M. Schick, WILEY-VCH, Weinheim, Germany, 2006, vol. 2, pp. 1–86.
8 E. Pouget, E. Grelet and M. P. Lettinga, *Phys. Rev. E: Stat., Nonlinear, Soft Matter Phys.*, 2011, **84**, 041704.
9 F. Tombolato, A. Ferrarini and E. Grelet, *Phys. Rev. Lett.*, 2006, **96**, 258301.
10 Z. Dogic and S. Fraden, *Langmuir*, 2000, **16**, 7820–7824.
11 S. Tomar, M. M. Green and L. A. Day, *J. Am. Chem. Soc.*, 2007, **129**, 3367–3375.
12 K. R. Purdy and S. Fraden, *Phys. Rev. E: Stat., Nonlinear, Soft Matter Phys.*, 2004, **70**, 061703.
13 J. X. Tang and S. Fraden, *Liq. Cryst.*, 1995, **19**, 459–467.
14 E. Barry, D. Beller and Z. Dogic, *Soft Matter*, 2009, **5**, 2563–2570.
15 E. Grelet and S. Fraden, *Phys. Rev. Lett.*, 2003, **90**, 198302.
16 E. Grelet, *Phys. Rev. Lett.*, 2008, **100**, 168301.
17 S. C. Glotzer and M. J. Solomon, *Nat. Mater.*, 2007, **6**, 557–562.
18 W.-J. Chung, J.-W. Oh, K. Kwak, B. Y. Lee, J. Meyer, E. Wang, A. Hexemer and S.-W. Lee, *Nature*, 2011, **478**, 364–368.
19 T. Gibaud, E. Barry, M. J. Zakhary, M. Henglin, A. Ward, Y. S. Yang, C. Berciu, R. Oldenbourg, M. F. Hagan, D. Nicastro, R. B. Meyer and Z. Dogic, *Nature*, 2012, **481**, 348–U127.
20 Y. Lin, E. Balizan, L. A. Lee, Z. Niu and Q. Wang, *Angew. Chem., Int. Ed.*, 2009, **49**, 868–872.
21 Z. Liu, J. Qiao, Z. Niu and Q. Wang, *Chem. Soc. Rev.*, 2012, **41**, 6178–6194.
22 D. A. Marvin, *Curr. Opin. Struct. Biol.*, 1998, **8**, 150–158.
23 K. Li, Y. Chen, S. Li, H. G. Nguyen, Z. Niu, S. You, C. M. Mello, X. Lu and Q. Wang, *Bioconjugate Chem.*, 2010, **21**, 1369–1377.
24 Y. S. Nam, T. Shin, H. Park, A. P. Magyar, K. Choi, G. Fantner, K. A. Nelson and A. M. Belcher, *J. Am. Chem. Soc.*, 2010, **132**, 1462–1463.
25 Z. Zhang, J. Buitenhuis, A. Cukkemane, M. Brocker, B. Bott and J. K. G. Dhont, *Langmuir*, 2010, **26**, 10593–10599.
26 K. Zimmermann, H. Hagedorn, C. C. Heuck, M. Hinrichsen and H. Ludwig, *J. Biol. Chem.*, 1986, **261**, 1653–1655.
27 Z. Dogic, J. Zhang, A. W. C. Lau, H. Aranda-Espinoza, P. Dalhaimer, D. E. Discher, P. A. Janmey, R. D. Kamien, T. C. Lubensky and A. G. Yodh, *Phys. Rev. Lett.*, 2004, **92**, 125503.
28 M. P. Lettinga, E. Barry and Z. Dogic, *Europhys. Lett.*, 2005, **71**, 692–698.
29 G. L. Li, Q. Wen and J. X. Tang, *J. Chem. Phys.*, 2005, **122**, 104708.
30 J. Sambrook and D. W. Russell, *Molecular Cloning: A Laboratory Manual*, Cold Spring Harbor Laboratory Press, New York, 3rd edn, 2001.
31 J. Armstrong, J. A. Hewitt and R. N. Perham, *EMBO J.*, 1983, **2**, 1641–1646.
32 S. A. Berkowitz and L. A. Day, *J. Mol. Biol.*, 1976, **102**, 531–547.
33 A. Waggoner, L. Taylor, A. Seadler and T. Dunlay, *Hum. Pathol.*, 1996, **27**, 494–502.
34 U. K. Laemmli, *Nature*, 1970, **227**, 680–685.
35 G. A. Griess, E. T. Moreno, R. Herrmann and P. Serwer, *Biopolymers*, 1990, **29**, 1277–1287.
36 B. D. Hamman, A. V. Oleinikov, G. G. Jokhadze, D. E. Bochkariov, R. R. Traut and D. M. Jameson, *J. Biol. Chem.*, 1996, **271**, 7568–7573.
37 B. Z. Packard, D. D. Toptygin, A. Komoriya and L. Brand, *Proc. Natl. Acad. Sci. U. S. A.*, 1996, **93**, 11640–11645.
38 B. Z. Packard, D. D. Toptygin, A. Komoriya and L. Brand, *J. Phys. Chem. B*, 1998, **102**, 752–758.
39 J. E. Selwyn and J. I. Steinfeld, *J. Phys. Chem.*, 1972, **76**, 762–774.
40 P. Serwer and S. J. Hayes, *Electrophoresis*, 1982, **3**, 76–80.
41 A. B. Harris, R. D. Kamien and T. C. Lubensky, *Rev. Mod. Phys.*, 1999, **71**, 1745–1757.
42 A. G. Cherstvy, *J. Phys. Chem. B*, 2008, **112**, 12585–12595.
43 H. H. Wensink and G. Jackson, *J. Chem. Phys.*, 2009, **130**, 234911.
44 Z. Zhang, N. Krishna, M. P. Lettinga, J. Vermant and E. Grelet, *Langmuir*, 2009, **25**, 2437–2442.
45 B. Willis, L. M. Eubanks, M. R. Wood, K. D. Janda, T. J. Dickerson and R. A. Lerner, *Proc. Natl. Acad. Sci. U. S. A.*, 2008, **105**, 1416–1419.
46 L. Rossi, S. Sacanna and K. P. Velikov, *Soft Matter*, 2011, **7**, 64–67.
47 L. Song, U. S. Kim, J. Wilcoxon and J. M. Schurr, *Biopolymers*, 1991, **31**, 547–567.
48 M. J. Glucksman, S. Bhattacharjee and L. Makowski, *J. Mol. Biol.*, 1992, **226**, 455–470.
49 W. M. Tan, R. Jelinek, S. J. Opella, P. Malik, T. D. Terry and R. N. Perham, *J. Mol. Biol.*, 1999, **286**, 787–796.

50 S. Bhattacharjee, M. Glucksman and L. Makowski, *Biophys. J.*, 1992, **61**, 725–735.
51 P. Schwind, H. Kramer, A. Kremser, U. Ramsberger and I. Rasched, *Eur. J. Biochem.*, 1992, **210**, 431–436.
52 G. Iannolo, O. Minenkova, R. Petruzzelli and G. Cesareni, *J. Mol. Biol.*, 1995, **248**, 835–844.
53 P. Malik, T. D. Tarry, L. R. Gowda, A. Langara, S. A. Petukhov, M. F. Symmons, L. C. Welsh, D. A. Marvin and R. N. Perham, *J. Mol. Biol.*, 1996, **260**, 9–21.
54 G. Kishchenko, H. Batliwala and L. Makowski, *J. Mol. Biol.*, 1994, **241**, 208–213.
55 P. Ilich, P. K. Mishra, S. Macura and T. P. Burghardt, *Spectrochim. Acta, Part A*, 1996, **52**, 1323–1330.
56 I. Moreno-Villoslada, R. Gonzalez, S. Hess, B. L. Rivas, T. Shibue and H. Nishide, *J. Phys. Chem. B*, 2006, **110**, 21576–21581.
57 Z. Dogic, K. R. Purdy, E. Grelet, M. Adams and S. Fraden, *Phys. Rev. E: Stat., Nonlinear, Soft Matter Phys.*, 2004, **69**, 051702.

Electronic Supplementary Information for:

Tuning chirality in the self-assembly of rod-like viruses by chemical surface modifications

Zhenkun Zhang [a,b] and Eric Grelet [*,b]

[a] *Key Laboratory of Functional Polymer Materials, Ministry of Education, Institute of Polymer Chemistry, Nankai University, Tianjin 300071, P. R. China.*

[b] *Université de Bordeaux et CNRS, Centre de Recherche Paul-Pascal, 115 Avenue Schweitzer, F-33600 Pessac, France.*

grelet@crpp-bordeaux.cnrs.fr

Mass spectrometry of the *fd* virus modified with methyl acetimidate (fd-MA)

The details for the sample preparation and MALDI-TOF mass spectrometry were the same as reported in the previous publications.[1] The band in the SDS-PAGE containing the modified coat protein, g8p, was subjected to CNBr cleavage which selectively breaks proteins at the carboxyl side of the methionine residue (position 21) of g8p (Fig. S1). It resulted two fragments: one is the *N*-terminal part (Fragment 1) and another *C*-terminal part (Fragment 2).

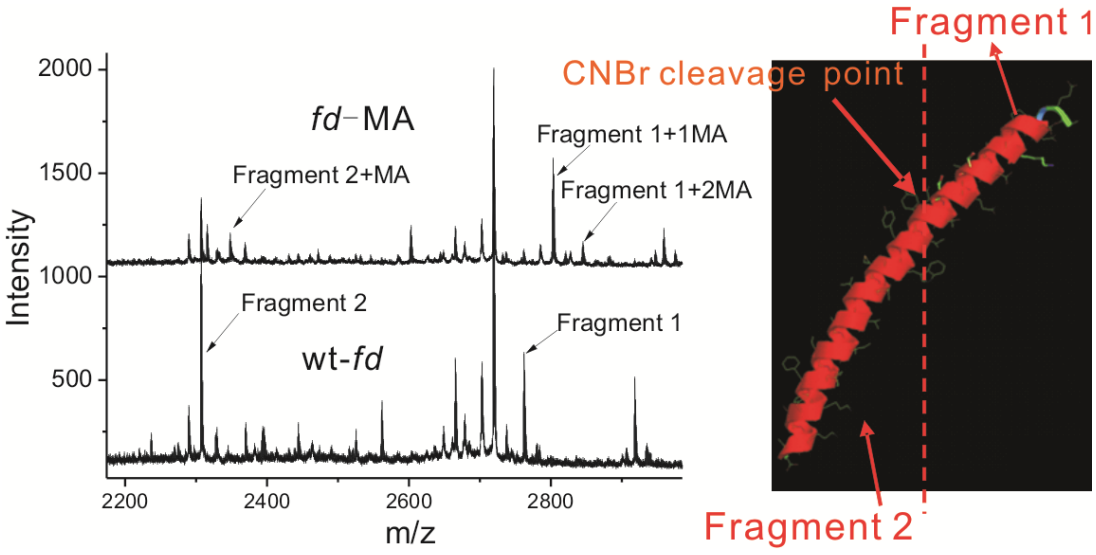

Figure S1. MALDI-TOF mass spectrometry of the coat protein of *fd*-MA after CNBr denaturation dividing the main coat protein into two fragments.

After being modified with MA, the peak in the spectrum of the wild-type *fd*, corresponding to the *N*-terminal part (Fragment 1), disappears while two new peaks appear which represent one modification (Fragment 1 plus 1 MA) and two modifications (Fragment 1 plus 2 MA) respectively. In addition, there is a peak corresponding to one modification in the *C*-terminal part (Fragment 2).

UV-visible spectra of *fd* viruses labeled with dyes (*fd*-FITC and *fd*-ROX)

For the UV-visible spectra, diluted solutions of the wild-type *fd* viruses, dye-labeled viruses and free dyes were prepared in TRIS-HCl NaCl buffer (I = 15 mM, pH 8.2). The UV-visible spectra were recorded on a Unicam UV-Vis spectrophotometer, with a scanning step of 2 nm, and are shown in Fig. S2.

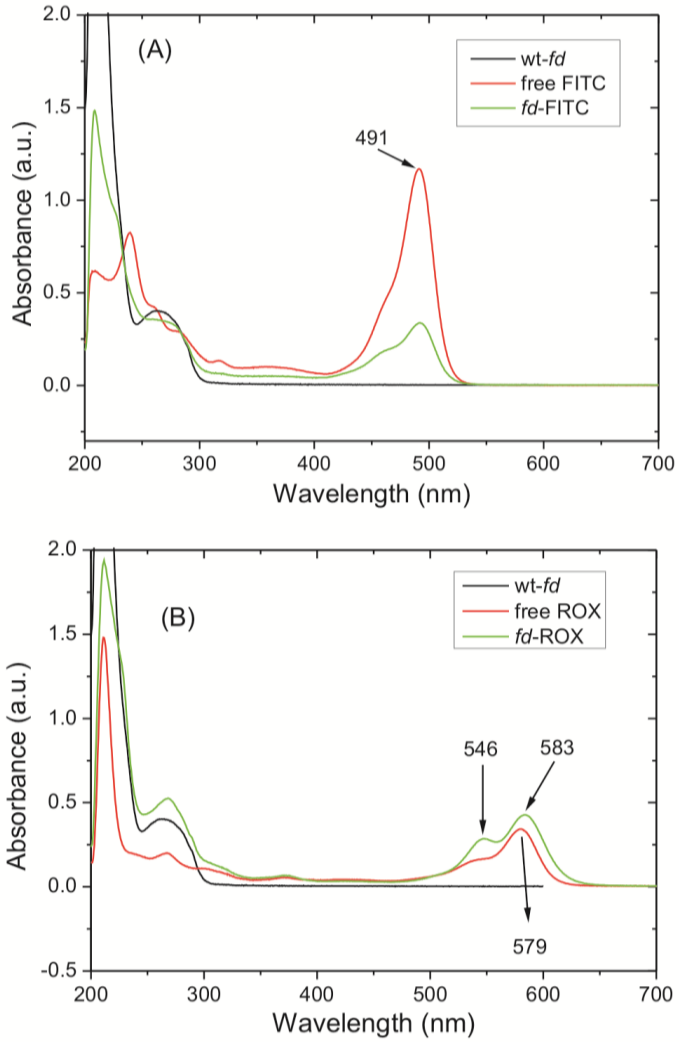

Figure S2. UV visible spectra of *fd* viruses labeled with dyes. (A) Comparison of the optical absorbance of FITC, wild-type *fd* virus and FITC labeled *fd* virus (*fd*-FITC). (B) Comparison of the absorbance of ROX, wild-type *fd* virus and ROX labeled *fd* virus (*fd*-ROX). The numbers represent the wavelength of the maximum of absorption.

Determination of A_{269}/A_{491} for pure FITC

A stock of FITC solution was prepared by dissolving FTIC in DMSO and then adding to TRIS-HCl-NaCl buffer (I=15 mM, pH 8.2). A set of samples obtained by dilution by mass with a concentration, C, ranging from 1 to 20 μg mL^{-1} were prepared in order to obtain the real concentration of the suspension of dye labeled viruses by determining the ratio, $a=A_{269}/A_{491}$. The absorption spectrum in the range from 200 to 700 nm was recorded with the use of spectrophotometer. The results are summarized in Fig. S3, and they show that the ratio *a* is independent of the dye concentration as expected.

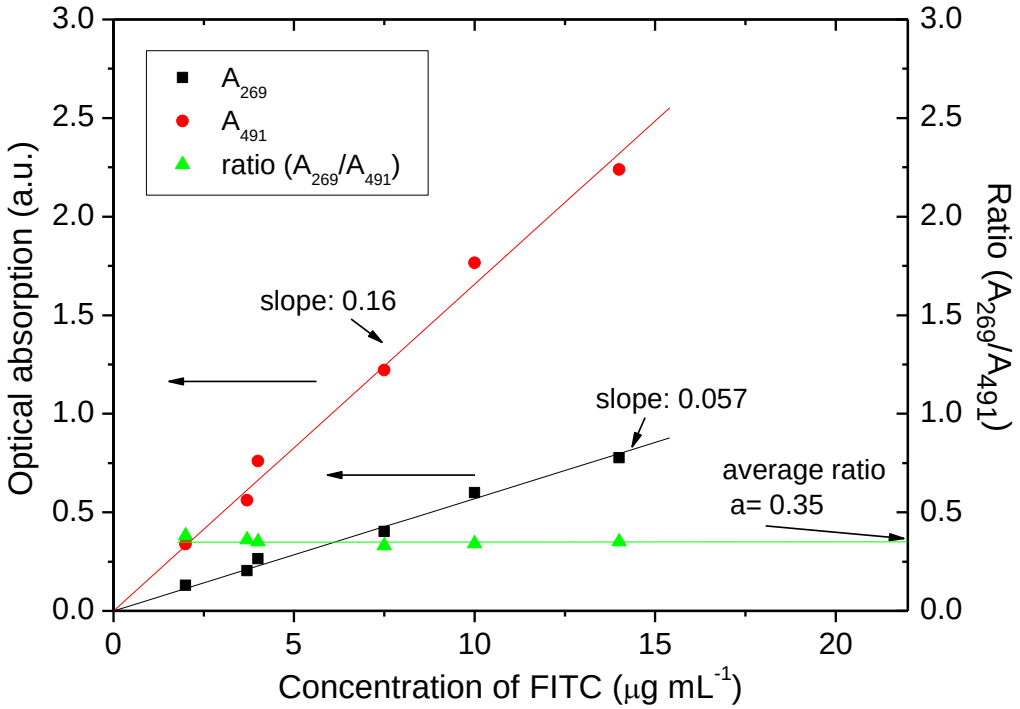

Figure S3. Absorptions of pure FTIC dye at varied concentrations.

Reference

1. Z. K. Zhang, J. Buitenhuis, A. Cukkemane, M. Brocker, B. Bott and J. K. G. Dhont, *Langmuir*, 2010, **26**, 10593-10599.